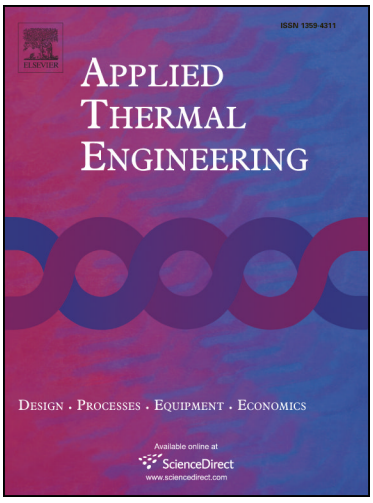

Nucleate pool boiling heat transfer of SES36 fluid on nanoporous surfaces obtained by electrophoretic deposition of Al_2O_3

Gu Song, Philip A. Davies, Jie Wen, Guoqiang Xu, Yongkai Quan

PII: S1359-4311(17)32012-4
DOI: https://doi.org/10.1016/j.applthermaleng.2017.12.068
Reference: ATE 11589

To appear in: *Applied Thermal Engineering*

Received Date: 26 March 2017
Revised Date: 24 November 2017
Accepted Date: 16 December 2017

Please cite this article as: G. Song, P.A. Davies, J. Wen, G. Xu, Y. Quan, Nucleate pool boiling heat transfer of SES36 fluid on nanoporous surfaces obtained by electrophoretic deposition of Al_2O_3, *Applied Thermal Engineering* (2017), doi: https://doi.org/10.1016/j.applthermaleng.2017.12.068

Nucleate pool boiling heat transfer of SES36 fluid on nanoporous surfaces obtained by electrophoretic deposition of Al_2O_3

Gu Song[a,c], Philip A. Davies[b#], Jie Wen[a], Guoqiang Xu[a], Yongkai Quan[a*]

[a] National Key Laboratory of Science and Technology on Aero-Engine Aero-thermodynamics, School of Energy and Power Engineering, Beihang University, Beijing 100191, China

[b] Aston Institute of Materials Research, School of Engineering and Applied Science, Aston University, Birmingham, B4 7ET, UK

[c] Shipbuilding Information Center of China, Beijing 100101, China

[#] Co-Corresponding author p.a.davies@aston.ac.uk

* Corresponding author quanyongkai@buaa.edu.cn

Abstract

With the aim of enhancing pool boiling heat transfer coefficient (HTC), the nucleate boiling performance of nanoporous surfaces obtained by an electrophoretic deposition (EPD) method is evaluated in this paper, with SES36 as the boiling fluid. A pool boiling experimental apparatus and procedure are described. Three kinds of experiment have been performed: (i) smooth stainless steel (SS) surface with pure SES36, providing the baseline; (ii) smooth SS surface with boiling nanofluid consisting of 0.5, 1 and 2 wt% Al_2O_3 suspended in SES36; (iii) nanoporous surfaces, of SS coated by EPD in procedures using 0.5, 1 and 2wt% concentrations of Al_2O_3, with pure SES36 as the boiling fluid. In (ii), the results show that the HTC of the smooth SS surface deteriorated with increasing concentration of Al_2O_3. In (iii), however, the HTC increased by approximately 6.2%, 30.5% and 76.9% for surfaces prepared with suspensions containing 0.5, 1 and 2 wt% Al_2O_3 respectively under the heat flux of 90 kW/m^2, compared with the baseline of the smooth surface in (i). The boiling behaviors are related to the modified surface micro-morphology due to the deposition of nanoparticles, as visualised by scanning electron microscopy (SEM).

The maximum active nucleation site density was about 2.6×10^5 sites/m^2 for the 2 wt% EPD surface under 94 kW/m^2, which is 1.8 times of the smooth SS surface. The increased site density of the nanoporous surface obtained by EPD enhanced greatly the nucleate pool boiling.

Keywords

Nucleate pool boiling; heat transfer coefficient; nanoporous surfaces; electrophoretic deposition; active nucleation site density

1. Introduction

Boiling is one of the most effective modes of heat transfer, providing high flux to meet the demands of many industrial applications including power plants, organic Rankine cycle (ORC), heat-exchanger systems, refrigeration systems and electronic device cooling systems [1]. As smaller and more powerful energy systems get developed, however, conventional boiling fluids are no longer adequate for their growing heat transfer demands [2]. Hence, modified pool boiling working fluids and boiling surfaces are important to further enhance heat transfer in such applications.

The use of nanoparticles in pool boiling processes is gaining more and more attention as a means of enhancing the heat transfer coefficient (HTC) [3-8]. In some studies, unmodified bare surfaces are used to boil nanofluids [9-12]; whereas in others, surfaces previously modified with nanoparticles are used to boil a pure working fluid [13-20]. Table 1 summarizes several of the key studies, and a brief overview of these follows.

Nanofluids are colloidal suspensions of nanoparticles in a base fluid. Addition of various nanoparticles – such as carbon nanotubes (CNTs), metal particles or metal oxide particles – generally increases the heat conductivity of the base fluid, suggesting that, even when boiling with bare surfaces, an increase of HTC should be possible. Indeed, Park et al. [9] observed up to 28.7% increase in HTC at low heat flux, when investigating the nucleate boiling of 1.0 vol% CNTs nanofluid with R22

and water as base fluids. In contrast, Trisaksri et al. [10] observed a deterioration in HTC when testing R141b nanofluid at different concentrations of TiO_2 with a cylindrical tube as the boiling surface. The boiling heat transfer curves were suppressed at higher concentration of nanoparticles. Vafaei [12] studied boiling with rough and smooth surfaces of copper with water and alumina nanofluids at different concentrations. The heated substrate was observed to be covered by a tiny porous layer of deposited nanoparticles that modified the size of cavities. The HTC was dependent on the relative size of these deposited nanoparticles and cavities in the rough surfaces. Therefore, use of bare surfaces to boil directly nanofluids has not always been successful in the enhancement of pool boiling heat transfer.

Gerardi et al. [11] combined both surface and fluid modification by studying the pool boiling of water-based nanofluids with diamond and silica nanoparticles on indium-tin-oxide surfaces. A series of fundamental parameters such as the bubble departure diameter and frequency, growth and wait times, were directly measured with the use of infrared thermometry. The results showed that the nanoparticles caused about 50% deterioration in the nucleate boiling heat transfer and about 100% increase in the critical heat flux (CHF). The improved surface wettability (due to the deposited porous layer during boiling) reduced the bubble departure frequency and nucleation site density, leading to deterioration in HTC.

Besides nanoparticle deposition, modifications like microchannels, microporous and nanostructure coatings on the boiling surface are also promising to enhance boiling heat transfer in many energy fields [21]. A number of research studies have been carried out to explore such modified surfaces using boiling pure working fluid. Launary et al. [13] studied silicon surfaces bare and fully coated with CNTs and 3D microstructures boiling with water and FC-72. The 3D microstructure exhibited the best performance, with the maximum heat flux reaching 270 kW/m^2 when boiling with FC-32. The CNT-enabled nano-structured interfaces improve heat transfer only at very low superheats. Sebastine et al. [14] also examined silicon substrates coated with CNTs boiling with FC-72. The positive results showed that the CNTs coating was highly effective at reducing the incipient superheat and greatly enhancing both

the HTC and the critical heat flux CHF. McHale et al. [16] compared 4 kinds of boiling surfaces including smooth copper with or without sintered copper particles, and then coated with CNT. The hybrid-sintered copper with CNT surface exhibited the best boiling performance for both fluids. Lee et al. [19] used plain surface and nano structured surface obtained by two-step anodizing. The results showed that nano structured surface have higher HTC than plain surface which is also consistent with the findings of references [14, 16].

Several other surface modification techniques have been tried. Tang et al. [17] used dealloying, Seongchul et al. [18] studied electrospun nanofibers, Lee et al. [19] adopted two-step anodizing and Dong et al. [20] performed a dry etching process to get micro-cavities on silicon surface. All these modified nano structured surface give a much higher HTC than smooth surfaces. But frequently they require complex processing, which is likely to be expensive in practice. In contrast, electrophoretic deposition (EPD) is a relatively simple technique that produces homogeneous nanofilms on a substrate, with great potential to modify surfaces and enhance the nucleate pool boiling. In EPD, charged nanoparticles dispersed in a liquid are attracted towards a conductive electrode of opposite charge, on which they deposit to form a permanent coating. Compared to other processes, EPD has advantages of easy control of process parameters, allowing substrates of complex shape to be coated; and it is a simple, low-cost process [22, 23]. Steven et al. [15] first used the EPD method to modify a surface and found 200% improvement in HTC. Further studies are needed to complement and complete this very promising method.

The base fluid is also the key factor in influencing the pool boiling. Solkatherm® SES36 [24, 25] is an azeotropic mixture of 65% R365mfc (1,1,1,3,3-pentafluorobutane) and 35% PFPE (perfluoropolyether), which boils at 36.7 °C. This new fluid can be used in direct contact cooling, heat pipes and ORC cycles for its excellent thermal physical properties. Boiling at lower temperature avoids the possible destruction of electronic of devices by excessive heat flux. It can also enable ORC cycles to work with smaller driving temperatures. Thus SES36 was selected as the boiling fluid for its great advantages of low boiling temperature,

thermal stability and non-toxicity.

The main aim of the present study was to measure the nucleate boiling performance of nanoporous surfaces modified by the EPD method with SES36 fluid. In an earlier study, it was shown that controllable dense films of nanoparticles can be created with the help of the Uniform Design method which is used to optimize the parameters of the EPD process [26]. The pool boiling experimental apparatus and detailed procedures are introduced. Three kinds of experiments are presented: first, smooth stainless steel (SS) surface boiling with pure SES36 fluid is performed to provide a baseline; second, smooth SS surface boiling with commonly used Al_2O_3 nanofluid (SES36 as base fluid) at concentrations of 0.5, 1 and 2 wt% are tested. Finally, nanoporous surfaces coated by EPD with 0.5, 1 and 2 wt% suspension concentrations boiling with pure SES36 are studied.

Table 1 A literature review of studies using nano particles and nanostructured surface (NSS) modification to enhance HTC, in chronological order

Author [reference]	Year	Nano structure and boiling surface	Working fluid	Remarks
Launary et al.[13]	2006	Carbon nanotubes (CNTs) Silicon surfaces bare and fully coated with CNTs 3D microstructures	PF5060(FC-72) Deionized water	● CNT-enabled NSS improved HTC only at very low superheats compared to smooth surfaces. ● Changes in the nature of surface-fluid interactions had negative effects on wetting.
Sebastine et al.[14]	2007	CNTs Silicon and copper substrates coated with CNTs	FC-72	➢ Full coating with CNT was very effective at reducing the incipient superheat, greatly enhancing both HTC and CHF. ➢ Greater enhancement achieved on Si than on Cu.
Park et al.[9]	2007	Plain tube	R22/Water based nanofluid with 1.0 vol% CNTs	● CNTs enhanced HTC with both R22 and water. ● Enhancement up to 28.7% at low fluxes. ● Enhancement suppressed at low fluxes - attributed to vigorous bubble generation.
Trisaksri et al.[10]	2009	cylindrical copper tube	R141b based nanofluid with 0.01, 0.03, 0.05 vol% TiO_2	➢ Boiling HTC deteriorated at high particle concentrations - especially at high fluxes. ➢ Boiling HTC was suppressed at 0.05 vol%.
Steven et al.[15]	2011	ZnO EPD SS surface	Deionized water	● 200% improvement in HTC was measured. ● Enhancement attributed to increased density of active nucleation sites. ➢ Infrared thermometry used to measure fundamental parameters such as the bubble departure diameter and frequency, growth and wait times.
Gerardi et al.[13]	2011	Indium-tin-oxide (ITO) film	Deionized water based nanofluid with 0.1 vol% Silica SiO_2 and 0.01 vol% Diamond C	➢ Nanoparticles reduced HTC by as much as 50%; but increased CHF by up to 100%. ➢ Deterioration in HTC attributed to decrease in bubble departure frequency and nucleation site density.

McHale et al. [16]	2011	CNTs Smooth copper Copper with sintered copper particles Smooth copper+CNTs Copper with sintered copper particles+CNTs	HFE-7300 Deionized water	● Hybrid sintered/CNT surface exhibited the best boiling performance for both fluids. ● No additional enhancement through the addition of CNTs on the sintered particle substrate. ● Hybrid surface achieved the lowest wall superheat at high fluxes with HFE-7300.
Tang et al.[17]	2013	Zn-Cu Nanoporous copper surface by dealloying	Deionized water	➢ 63.3% decrease in wall superheat and 172.7% increase in HTC observed. ➢ Thermal conductivity of nanostructure considered to play an important role in enhancing boiling, especially at high fluxes.
Seongchul et al.[18]	2013	Cu Copper platelets covered with copper-plated electrospun nanofibers	Ethanol Water	● HTC of NSS 3-8 times greater than with bare surfaces. ● NSS of copper-plated nanofibers facilitated bubble growth rate and increased bubble detachment frequency.
Lee et al.[19]	2014	Plain Surface (PS) Nano-structured surface (NSS)	LiBr Sodium Dodecyl Sulfate (SDS) Water	➢ NSS with water and LiBr have higher HTC than PS. ➢ Under SDS boiling conditions, HTC was increased on the PS, decreased on the NSS, compared with under pure water boiling conditions. ➢ Surface tension and surface wettability are the important parameters affecting the boiling heat transfer performance, should be taken into account.
Dong et al.[20]	2014	Silicon chips with micro-pillars (MP), micro-cavities (MC), nanowires (NW) and nano-cavities (NC).	Ethanol	● Microstructures enhanced bubble nucleation by significantly increasing the active nucleation site density at low heat fluxes. ● At high fluxes corresponding to critical conditions, nano-structures delayed bubbles from merging, preventing

Vafaei [12]	2015	Copper surface with roughness of 420 nm and 25nm	Deionized water based nanofluid with 0.001, 0.01, 0.1 vt% δ-Al_2O_3	the vapor film from spreading. ➢ HTC depended on cavity size and wettability but also on the range of heat flux. ➢ At low fluxes, big cavities were active in initiating nucleation; small cavities active only at high fluxes. ➢ Suspended nanoparticles concluded to have 'a great potential to modify the radius of triple line, waiting, bubble formation times and bubble frequency'.

2. Experimental and methods

In this section, the preparation of nanoporous surface modified by electrophoretic deposition method is presented. Then the pool boiling experimental apparatus and procedure are explained in detail. Finally, data calculation and measurement uncertainty are presented.

2.1. Boiling surface prepared by EPD

Gamma-phase aluminum oxide nanopowder (γ-Al_2O_3, Sigma-Aldrich product number 544833) was used as the coating material in this study. It was used to coat 304 stainless-steel discs of diameter 40 mm and thickness 3 mm. To produce the nanoporous surface, the EPD process was carried out in three steps: pretreatment of base material, preparation of nanofluid, and the EPD process. The key characteristics of the coated nanoporous surface, including thickness and morphology, depend on many parameters like suspension concentration, deposition time, applied voltage and suspension pH. The detailed procedure used was the same as that reported in a previous study in which EPD were optimized using the uniform design approach [26]. Three suspension concentrations (0.5, 1 and 2 wt%) of Al_2O_3 were used to explore the effect on HTC performance.

2.2. Experimental apparatus and procedure

The nucleate pool boiling apparatus consisted of heating, evaporating and condensing sections, as shown schematically in Fig. 1. The design was adapted from that described in reference [15]. A cartridge heater (150 W, 230 V) was inserted into a copper rod to generate heat flux from electrical power supply, which was adjustable by means of an electrical transformer. The stainless steel disc was heated by heat flow coming from the copper rod and then passing through the nanoporous surface thus boiling the organic fluid, which was contained in a polycarbonate tube. To reduce radial heat losses and make sure the heat flow in one-dimensional as possible, the copper rod and stainless steel disc were encased by a 50 mm outside diameter polytetrafluoroethylene (PTFE) cylinder. The polycarbonate tube had a 50 mm diameter flange housing an O-ring seal between the boiling fluid and heating section. To

maintain constant liquid level, a reflux condenser was inserted through the aluminum plug at the top of the polycarbonate tube. All parts of the rig were held together by 4 long bolts through flanges on the top and bottom aluminum plugs. Joints were sealed by elastic sealant.

The temperature of the copper rod was measured by three type-K thermocouples spaced 20 mm apart axially. As the temperature of the boiling surface is difficult to measure directly, a type-K thermocouple was fixed at the middle hole of the stainless steel disc. The temperature of top boiling surface was calculated with the use of steady-state heat conduction formula. The wires of the four thermocouples (resistant to high temperature) were inserted in the middle of the copper rod and stainless steel disc through 2 mm diameter holes in the PTFE insulation. And the saturation temperature of fluid was measured by an armored type-K thermocouple immersed in the liquid through the hole of the top aluminum plug. The five thermocouples were toleranced to Class 1 accuracy, the error limit to ±0.75%t. All temperature values were recorded by a data logger (Pico Technology USB TC-08). The input heating power, voltage and current were recorded by a multifunctional power meter (HOBUT M850-MP1). The smooth stainless steel and coated nanoporous surfaces were examined for morphology by a scanning electron microscope (SEM). The 3D-shape and roughness of deposited surfaces were measured at the nanoscale by an atomic force microscope (AFM, Bruker dimension 3100).

The nucleate pool boiling performance of SES36 with different boiling surfaces, including the effect of nanoparticles, was tested to explore the enhanced HTC method and extend the potential applications. The properties of SES36 are given in Table 2. The design of experiments is summarized in Table 3.

In a typical experiment, the boiling disc was placed onto the copper bar and 4 thermocouples were connected through the PTFE holes. All remaining parts were assembled and the 4 bolts tightened to get a good seal. The boiling fluid was injected from the top hole of the aluminum plug. After that, the reflux condenser was installed and cooling water was pumped in. The fluid was preheated to the saturated temperature by turning on the power supply. When bubbles began to appear in the polycarbonate tube, the power input value was fixed and time was allowed for the system to reach steady state, which was defined as the change of temperature less than 0.2 ℃ in 10 minutes. This typically took approximately 20

minutes. Time and the TC temperatures were automatically recorded, and the voltage value increased for the next heat flux state point. All the experiments were performed twice to reduce the influence of random error.

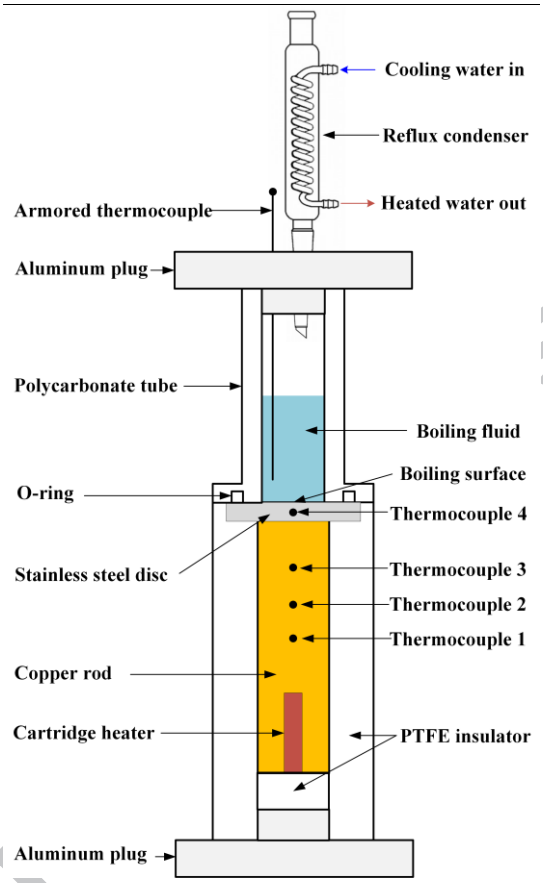

Fig 1 Schematic of nucleate pool boiling experimental facility

Table 2 Properties of SES36 fluid

Property	Unit	
Composition	-	Azeotropic mixture
Average molecular weight	kg/kmol	184.5
Boiling point at 1.013 bar	℃	35.6
Critical temperature	℃	177.6
Critical pressure	MPa	2.85
Density (saturated at 25 ℃)	kg/m^3	1365.4
Specific heat capacity (at 25 ℃)	kJ/kg K	1.21
Heat of vaporization (at 25 ℃)	kJ/kg	129.2

Table 3 The design of experiments

	Surface	Fluid	Wt%
1	Smooth stainless steel	SES36	pure
2	Smooth stainless steel	Al_2O_3 + SES36 nanofluid	0.5, 1, 2 wt%
3	0.5, 1, 2 wt% EPD nanoporous	SES36	pure

2.3. Calculation and measurement uncertainty

Heat flux (q) of the system was calculated using the following equation:

$$q = -k_c \frac{dT}{dx} = k_c \frac{T_1 - T_3}{2L} \tag{1}$$

where T_1 is the temperature measured of thermocouple 1 (near the cartridge heater, as shown in Fig. 1) and T_3 is the temperature measured of thermocouple 3 (near the boiling surface), k_c is the thermal conductivity of copper rod, 398 W/m K, and L is the spacing among thermocouples 1, 2 and 3 (L=20 mm).

The boiling surface temperature (T_w) is calculated as follows:

$$T_w = T_4 - \frac{qL_1}{2k_{ss}} \tag{2}$$

where T_4 is the temperature measured of thermocouple 4, k_{ss} is the thermal conductivity of stainless steel, 17 W/m K, and L_1 is the thickness of stainless steel disc, 3 mm.

And the superheat (ΔT_s) is given by:

$$\Delta T_s = T_w - T_{sat} \tag{3}$$

where T_{sat} is the directly measured saturation temperature of boiling fluid.

The average boiling heat transfer coefficient (h_b) is defined as:

$$h_b = \frac{q}{\Delta T_s} \tag{4}$$

A detailed uncertainty analysis of q (u_q), ΔT_s ($u_{\Delta Ts}$) and h_b (u_{hb}) performed in accordance with Moffat [27] gives the following:

$$u_q = \sqrt{\left(\frac{\delta q}{\delta k_c} u_{k_c}\right)^2 + \left(\frac{\delta q}{\delta T_1} u_{T_1}\right)^2 + \left(\frac{\delta q}{\delta T_3} u_{T_3}\right)^2 + \left(\frac{\delta q}{\delta L} u_L\right)^2} \tag{5}$$

$$u_{\Delta T_s} = \sqrt{\left(\frac{\delta \Delta T_s}{\delta T_w} u_{T_w}\right)^2 + \left(\frac{\delta \Delta T_s}{\delta T_{sat}} u_{T_{sat}}\right)^2} \tag{6}$$

$$u_{h_b} = \sqrt{\left(\frac{\delta h_b}{\delta q} u_q\right)^2 + \left(\frac{\delta h_b}{\delta \Delta T_s} u_{\Delta T_s}\right)^2} \tag{7}$$

The results show that the maximum relative uncertainty in heat flux u_q/q was 4.3%, the maximum relative uncertainty in superheat $u_{\Delta Ts}/\Delta T_s$ was 6.9% and the maximum relative

uncertainty in HTC u_{hb}/h_b was calculated to be less than 8.2%.

3. Experimental results

In this section, the results of the nucleate pool boiling heat transfer experiments are compared among the different surfaces and nanofluids used, and against an established correlation from the literature.

3.1. Comparison of experimental data with existing correlations

The classic correlation proposed by Cooper [28] was chosen because it is based on a large range of experiment data and is widely used to predict nucleate pool boiling heat transfer. The Cooper correlation takes the property of boiling surface roughness into account and is appropriate for the prediction of water, refrigerant and organic fluids; it has the following form:

$$\frac{h_b}{q^{0.67}} = 55\left(P_r\right)^{\left(0.12-0.2\log_{10} R_a\right)}\left(-\log_{10} P_r\right)^{-0.55} M^{-0.5} \tag{8}$$

where R_a is surface roughness (μm), P_r is reduced pressure defined as P/P_c and M is molecular weight, kg/kmol. As the correlation is valid for the boiling of pure fluid, tests of smooth SS surface boiling with pure SES36 were performed for comparison with the correlation. The tests were performed in duplicate for additional accuracy, referred to as Expt.1 and Expt.2.

As can be seen in Fig 2, results of heat transfer coefficient vs. superheat repeated well between duplicates, except for some divergence (Expt.2 showed a slightly higher heat flux than Expt.1 under the same superheat) when superheat was above 15 ℃. The experimental results show a very similar trend to the predictions of Cooper, though they are consistently slightly higher than the predictions. Considering the complexity of pool boiling heat transfer, and the inherent limitations of empirical correlations such as that of Cooper, the similar trends of the pool boiling curves tend to confirm the validity of the present experimental methods and results.

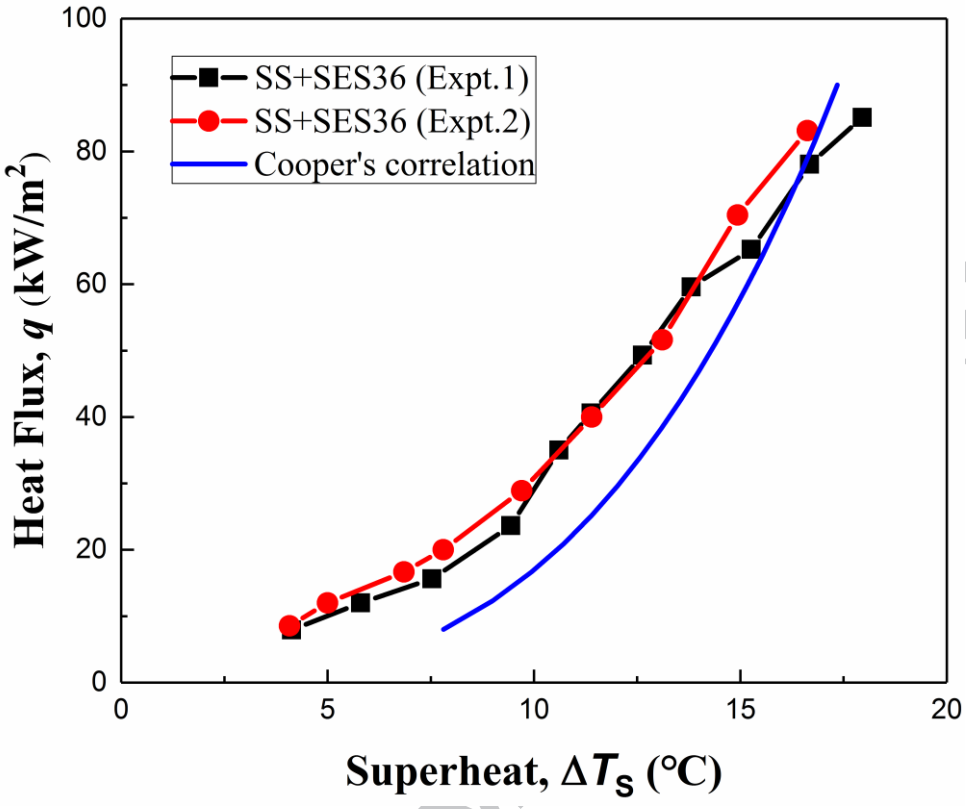

Fig 2 Comparison of pool boiling curve of experimental results (duplicated) with Cooper's correlation for SS surface boiling with SES36

3.2. Experimental results of smooth SS surface boiling with SES36 nanofluid

The experimental results of smooth SS surface boiling with SES36 nanofluid with 0.5 wt%, 1 wt% and 2 wt% Al_2O_3 particles are shown in Fig. 3. The experimental data (average of two runs) of smooth SS boiling with pure SES36 fluid are used as the baseline, based on polynomial fitting. As shown in Fig.3, the experimental results gave good repeatability within each pair of experiments. Compared with the baseline, the nucleate pool boiling heat transfer of nanofluid deteriorates with concentration. This finding agrees with many reports in the literature [10, 11]. Fig. 3a shows that the incipient boiling point increase with concentration, occurring at approximately 6 ℃, 8.5 ℃ and 11.3 ℃ for 0.5 wt%, 1 wt% and 2 wt% nanofluid, respectively. Correspondingly the HTC decreased by approximately 13.7%, 23.8% and 33.8% respectively, compared with the baseline of pure SES36 as shown in Fig. 3b. The experimental results indicate, therefore, that smooth SS surface boiling the nanofluid directly is not a good method to enhance the boiling heat transfer.

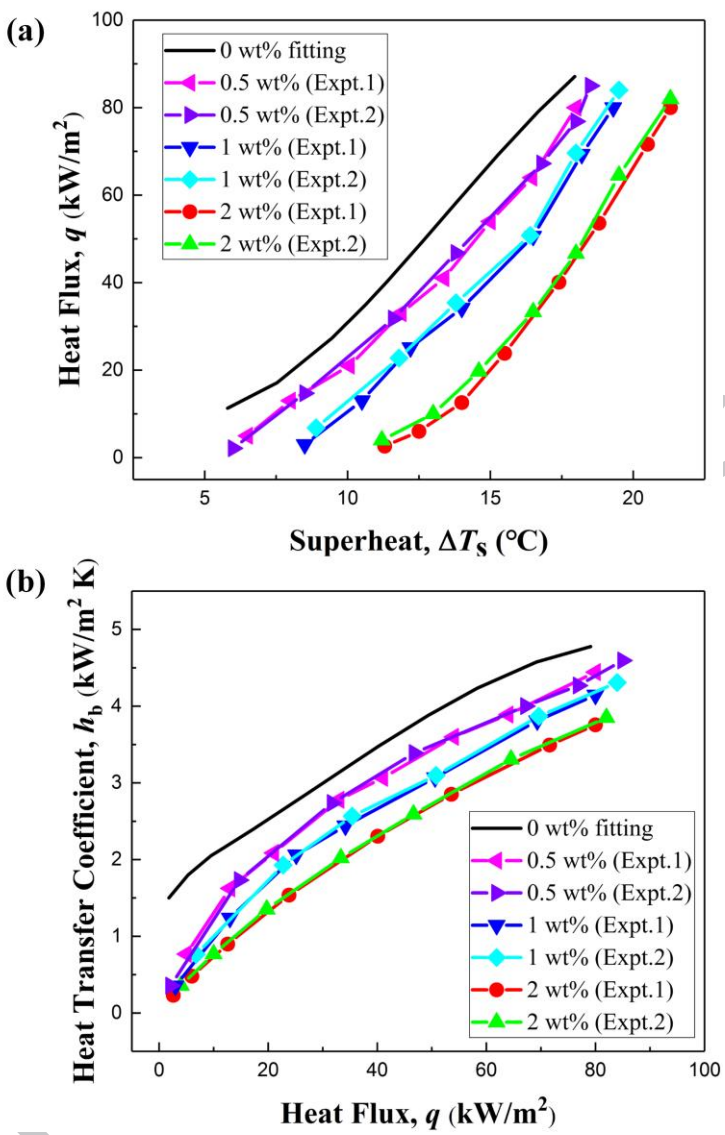

Fig 3 Experimental results of SS boiling with SES36 nanofluid (a) pool boiling curve (b) average heat transfer coefficient versus heat flux

3.3. Experimental results of EPD nanoporous surface boiling with SES36

The experimental results of EPD nanoporous surface boiling with pure SES36 are shown in Fig. 4. Compared with the baseline of pure SES36, the nucleate pool boiling heat transfer of pure SES36 fluid increased markedly with EPD concentration. Fig. 4a shows no significant difference of the incipient boiling point among all tests. But, the slope of pool boiling curve was quite different; the 2 wt% EPD case is steepest. At the maximum heat flux of 90 kW/m^2, the HTC increased by approximately 6.2%, 30.5% and 76.9% for 0.5 wt%, 1 wt% and 2 wt% EPD nanoporous surfaces respectively, against the baseline of pure SES36

(Fig. 4b). It should be noted that there is no linear relationship between the enhanced HTC here and EPD concentration. The higher the EPD concentration, the better the HTC. The experimental results show clearly that EPD nanoporous surface can increase heat transfer coefficient by a factor of up to 2, depending on the experimental parameters.

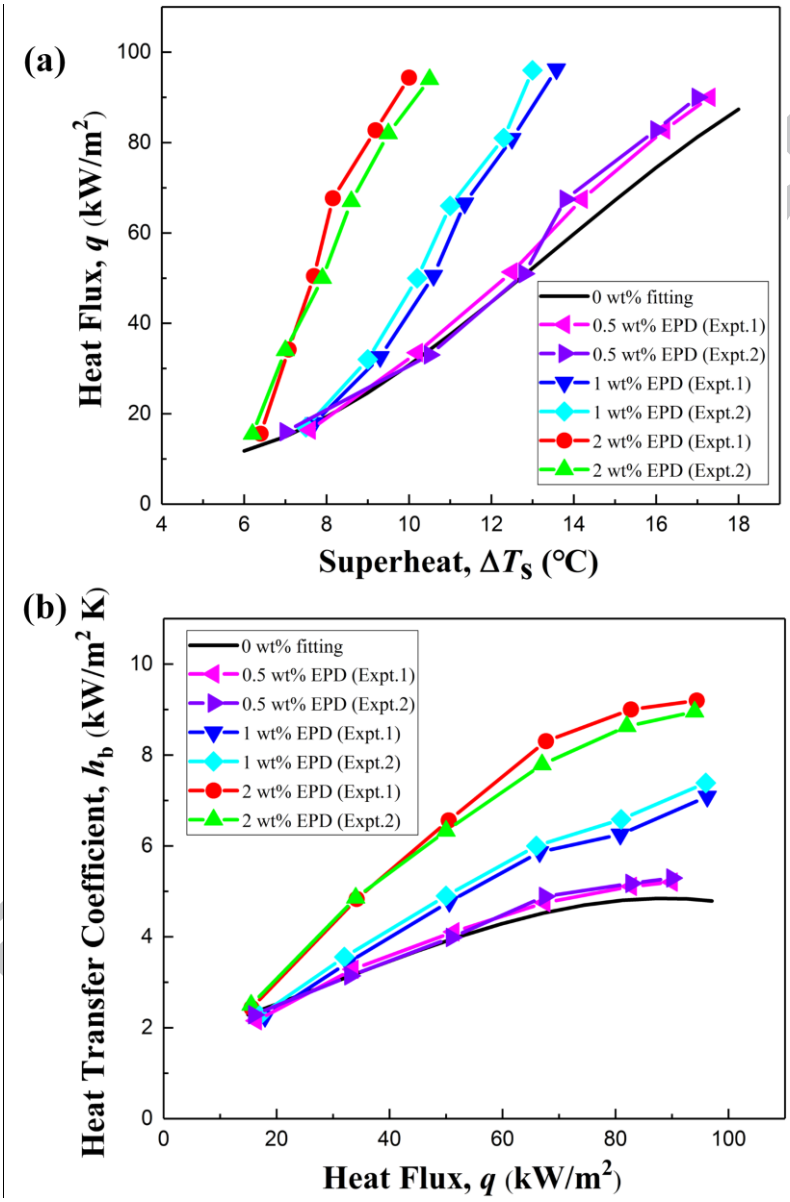

Fig 4 Experimental results of EPD nanoporous surface boiling with SES36 (a) pool boiling curve (b) average heat transfer coefficient versus heat flux

4. Results interpretation and discussion

As seen above, the nucleate pool boiling HTC of smooth SS surface boiling with SES36 nanofluid was found to decrease, while that of EPD nanoporous surface boiling with pure SES36 was found to increase, as compared to the baseline. These behaviors are

compatible and related to the modified surface micro-morphology due to the deposition of nanoparticles.

4.1. Scanning electron microscopy of nanoporous surface after boiling

Fig. 5 shows photographs and SEM images of the smooth SS surface with deposition after boiling with the nanofluid. The depth and amount of nano deposition layer on the SS surface increased with the nanofluid concentration. As can be seen from SEM images, nanoparticles accumulate as balls with a minimum diameter of about 1 μm compared to the mean size of Al_2O_3 particle is 50 nm. This suggests that substantial agglomerates formed during boiling. One possible reason is that most organic fluids (including SES36) are not the perfect base fluid for nanoparticles because of their polar properties. Even though stirring and ultrasonication were performed, the nanoparticles separated from the fluid and deposited on the bottom during the violent pool boiling process. This kind of deposition increases the thermal resistance of boiling surface and blocks the heat transfer. That is why the HTC of smooth SS surface boiling with SES36 nanofluid deteriorated, and the boiling curve moved to the right with the concentration increase - as shown in Fig. 4.

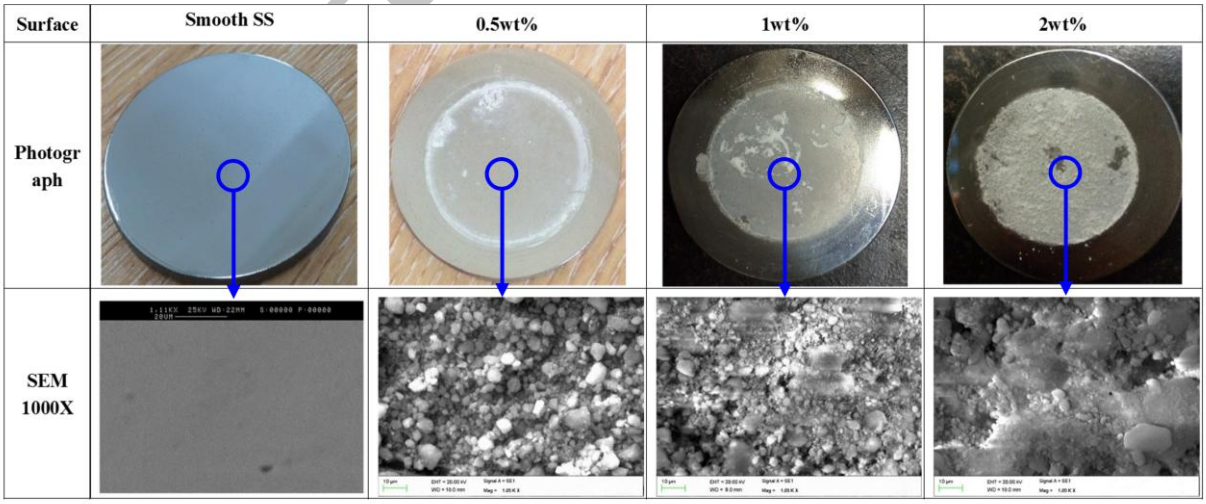

Fig 5 Photographs and SEM images of SS surface with deposition after boiling nanofluid

Fig. 6 shows photographs and SEM images of the EPD nanoporous surface before and after boiling with pure SES36 fluid. Note that, to protect the delicate surface and make sure the boiling process was not affected, these samples were not subject to SEM before boiling, SEM was carried out only after the boiling tests. As can be seen from the photographs, Al_2O_3

nanofilms were deposited compactly and uniformly on all the EPD surfaces regardless of the concentrations used in their preparation. After boiling, the bulk nano layer had flaked off and thinned due to the strong scouring action of the bubbles, and the higher the concentration of EPD, the more flaking occurred. But there are still enough residual film covering the SS surface, which primarily governed the boiling performance [15]. The SEM images show that the nanoporous layer, obtained by the EPD method on the SS surface, was uniform and no obvious agglomerates formed. This is because the Al_2O_3 nanofluid used in EPD process is water, providing a better dispersant compared to organic fluid. A myriad of nanopores on the boiling surface provides numerous active nucleation sites, greatly enhancing nucleate boiling HTC. On the other hand, the nanoporous layer may also increases the thermal resistance of boiling surface as the deposition of directly nanofluid boiling. Nonetheless, the end results demonstrate that the increase of active nucleation site density is dominant compared with the increase of thermal resistance.

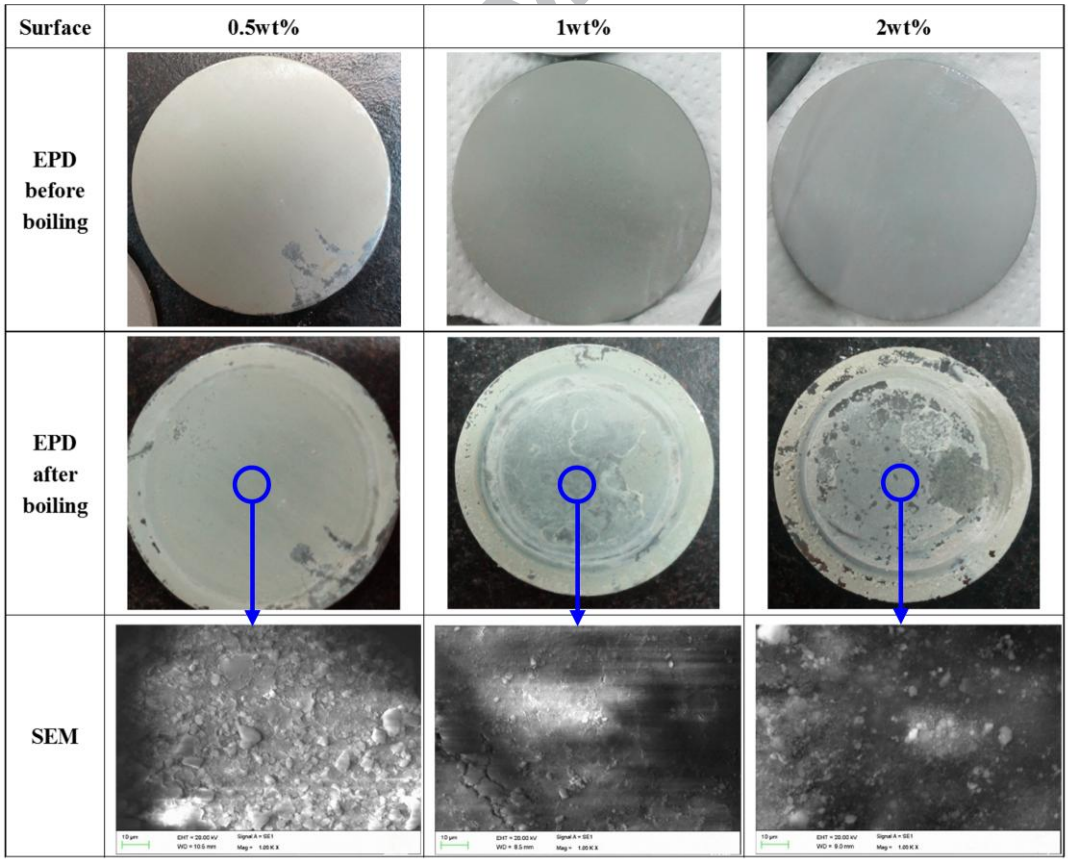

Fig 6 Photographs and SEM images of EPD nanoporous surface before and after boiling SES36

4.2. Surface roughness of nanoporous surface after boiling

The average surface roughness (R_a) affects the heat transfer coefficient because of its effect on vapour bubble growth. The HTC is expected to be proportional to R_a^m at a fixed heat flux, as proposed by Jones et al. [29], where m is an exponent defined by the boiling fluid and other parameters. It is therefore expected that the increase surface roughness should lead to a substantial enhancement of HTC.

Actually, the relationship between HTC and surface roughness is also implicit in equation 8. Here we investigated the variation in surface roughness, R_a with HTC under different heat flux, q, as shown in Fig. 7. The results show that the heat transfer coefficient enhanced as the roughness increased, which is consistent with Jones's conclusion. And the decreasing slope indicated that the exponent m should be less than 1 if the Jones' proportionality holds true. Moreover, the HTC also increased as the heat flux changed from 30 to 90 kW/m^2.

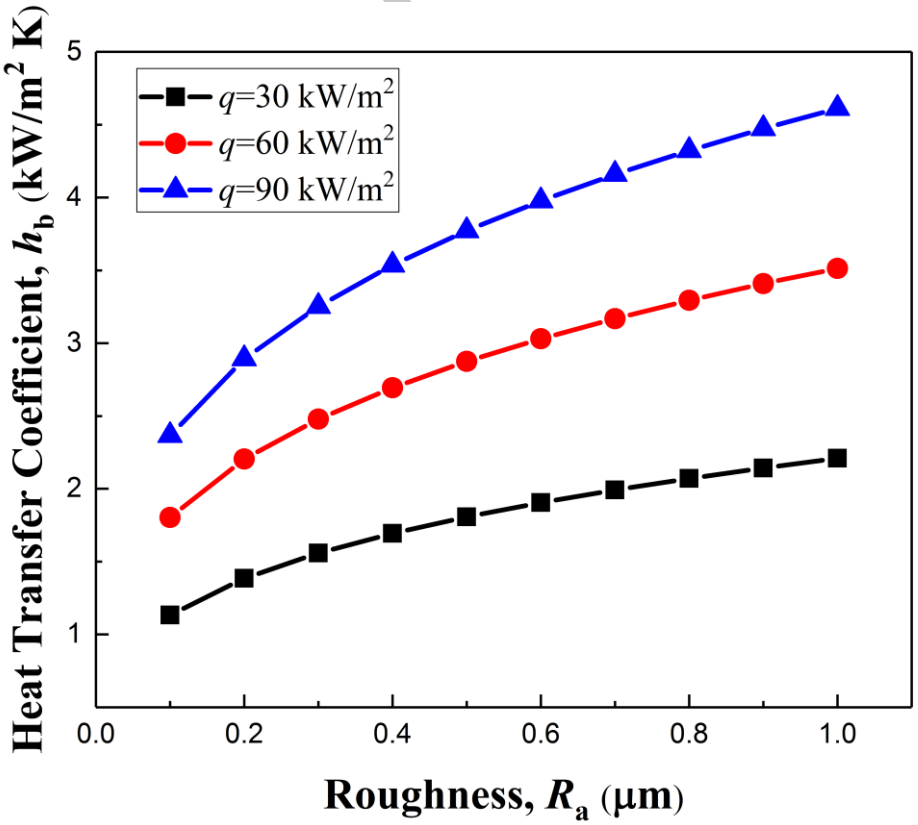

Fig 7 Variation in surface roughness with HTC based on Cooper's correlation

The average surface roughness after boiling was also investigated by AFM. As the pairs of experiments for the same case repeated well, the mean value of the roughness for each

case is given in Table 4. Considering the roughness of smooth stainless steel surface is 21.4 nm [26], nanoparticle deposition increases the roughness approximately from 8 to 25 times. Due to the peak-and-valley structure of the deposit, the vapour bubble growth will be affected dramatically. And the roughness of deposition surface boiling with nanofluid is higher than EPD surface for its agglomerates. The changes in roughness led to a great increase of HTC. The maximum HTC increased approximately 76.9% for 2wt% EPD nanoporous surface compared with the smooth SS boiling pure SES36. However, the final HTC of smooth SS surface boiling with nanofluid turns out to be deteriorated even despite the higher roughness compared to boiling with pure fluid. The poor heat transfer between disordered nano films and SS surface reduce the HTC is discussed in section 4.1. It suggested that the end results of pool boiling is always a tradeoff between many key parameters such as the surface roughness, heat transfer in boiling surface and active nucleation site density.

Table 4 The roughness of boiling surfaces

Surface	Wt%	R_a (nm)
Deposition after boiling with nanofluid	0.5	245.9
	1	389.5
	2	501
EPD after boiling with SES36	0.5	165.3
	1	192.5
	2	219.5

4.3. Active nucleation site density of EPD nanoporous surface after boiling

As mentioned above, active nucleation site density of boiling surface is the key parameter influenceing the pool boiling performance. But it is impractical to measure this parameter directly. A widely used boiling model, known as the Mikic-Rohsenow correlation, can be used to infer the number of nucleation sites [15, 30]:

$$q = \frac{1}{2}\left(\pi k_l \rho_l C_p\right)^{1/2} f^{1/2} D_d^2 n \Delta T_s \tag{9}$$

Where n is the nucleation site density in sites/m^2, k_l, ρ_l, C_p the fluid heat conductivity, density and the fluid specific heat respectively. D_d is the bubble departure diameter defined by equation 10 and f is the departure frequency defined by equation 11:

$$D_d = C_1 \left[\frac{\sigma}{(\rho_l - \rho_v)} \right]^{1/2} \left(\frac{\rho_l C_p T_{sat}}{\rho_v h_{fg}} \right)^{5/4} \tag{10}$$

$$fD_d = C_2 \left[\frac{\sigma(\rho_l - \rho_v) g}{\rho_l^2} \right]^{1/4} \tag{11}$$

where C_1 and C_2 are experimental constants: C_2=0.6 s/m$^{1/2}$; C_1=1.5×10^{-4} m$^{1/4}$s$^{3/2}$ for water, and C_1=4.65×10^{-4} m$^{1/4}$s$^{3/2}$ for other fluids [31].

Rearranging equation 9 for n:

$$n = \frac{2q}{(\pi k_l \rho_l C_p)^{1/2} f^{1/2} D_d^2 \Delta T_s} \tag{12}$$

Using equation 12 to calculate n for the EPD nanoporous surface boiling experiments in section 3.3 yields the results of Fig. 8 below showing how nucleation site density increases with heat flux q. Here the properties of SES36 given by the engineering equation solver (EES) at 35.6 ℃ [32].

The active nucleation site density increases with heat flux as shown in Fig. 8. The site density line of the pairs of 0.5 wt% EPD surface almost coincides with the baseline of smooth SS surface although it is slightly increased at heat flux higher than 50 kW/m^2. In comparison the site density of 1 and 2 wt% EPD surface are much bigger, suggesting that the number of nucleation sites increases with deposition weight. The maximum site density was about 2.6×10^5 sites/m^2 for the 2 wt% EPD surface under 94 kW/m^2, which is 1.8 times of the smooth SS surface. Considering the conclusion in section 3.3 that the HTC increased by approximately 76.9% for 2 wt% EPD nanoporous surface compared with the baseline of smooth surface, we infer that the number of active nucleation site density plays a crucial role in the value of boiling HTC. The increased active nucleation site density of the nanoporous surface obtained by EPD enhances the nucleate pool boiling greatly.

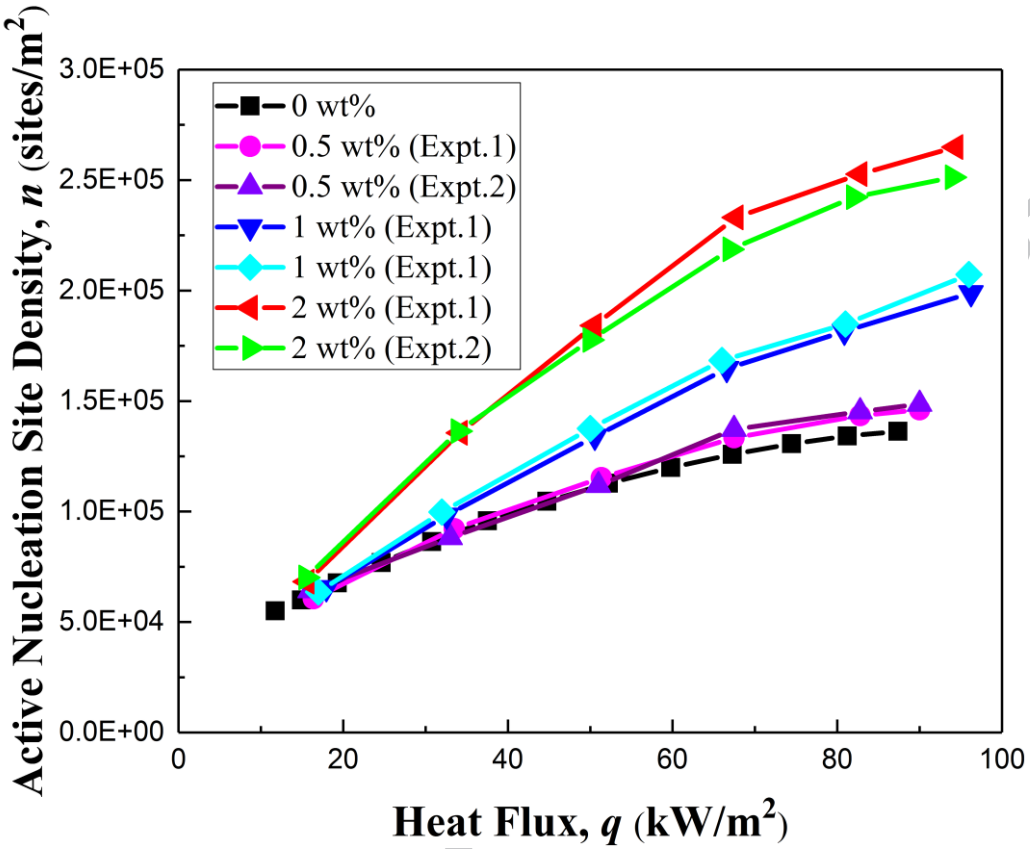

Fig 8 Variation in heat flux with active nucleation site density of EPD nanoporous surface after boiling

5. Conclusions

This work has explored the nucleate boiling performance of nanoporous surfaces modified with Al_2O_3 by the EPD method, with SES36 as the boiling fluid. A pool boiling experimental apparatus and procedure have been described. Three kinds of experiments have been conducted and the novel aspects of this work are as follows.

(1). The EPD surface was prepared by optimized parameters using the Uniform Design method. Uniform Design is a new method of experimental design that has been applied successfully in other fields, but not previously to the field of surface coatings for boiling enhancement.

(2). Tests of EPD surface boiling with pure fluid and SS surface boiling with nanofluid were performed and compared.

(3). The boiling characteristic of the azeotropic fluid SES36 was evaluated. This fluid is of increasing importance for application in low-temperature power cycles and relatively few

studies have been done on its detailed boiling properties. The superheat temperatures in nucleate boiling, as studied here, are particularly important as regards the low temperature differentials used in such cycles and are shown to be reduced substantially by EPD surface modification..

The main findings and conclusions of this work are as follows:

- The HTC of smooth SS surface boiling the nanofluid directly deteriorates with concentration of Al_2O_3 in the nanofluid. HTC decreased approximately 13.7%, 23.8% and 33.8% for 0.5 wt%, 1 wt% and 2 wt% nanofluid respectively, compared with the baseline of pure SES36.
- The HTC increased by approximately 6.2%, 30.5% and 76.9% for EPD nanoporous surface prepared at 0.5 wt%, 1 wt% and 2 wt% respectively under the heat flux of 90 kW/m^2, compared with the baseline of pure SES36. The experimental results show that EPD nanoporous surface can improve the pool boiling heat transfer of SES36 fluid greatly.
- The boiling behaviors are related to the modified surface micro-morphology due to the deposition of nanoparticles. A myriad of nanopores on the boiling surface forms numerous new cavities, which increase active nucleation site density.
- The maximum active nucleation site density was about 2.6×10^5 sites/m^2 for the 2 wt% EPD surface under 94 kW/m^2, which is 1.8 times of the smooth SS surface. The increased site density of nanoporous surface obtained by EPD enhances the nucleate pool boiling greatly.
- Future research effort is recommended to optimize the EPD deposition, to make it more stable for practical applications.

Acknowledgements

The authors would like to thank the Academic Excellence Foundation of BUAA for their financial support. GS thanks the China Scholarship Council (CSC, NO.201406020031) for a scholarship hosted at Aston University.

Nomenclature

C_p	specific heat (kJ/kg K)	*Abbreviations*	
C_1	experimental constants ($m^{1/4}s^{3/2}$)	AFM	atomic force microscope
C_2	experimental constants ($s/m^{1/2}$)	CHF	critical heat flux
D_d	bubble departure diameter	CNTs	carbon nanotubes
f	departure frequency	EES	engineering equation solver
g	gravitational acceleration (m/s^2)	EPD	electrophoretic deposition
h_b	boiling heat transfer coefficient (W/m^2 K)	HTC	heat transfer coefficient
h_{fg}	latent heat of vaporization (kJ/kg)	ORC	organic Rankine cycle
k	thermal conductivity (W/m K)	PTFE	polytetrafluoroethylene
L	displacement (m)	SEM	scanning electron microscopy
M	molecular weight (kg/kmol)	SS	stainless steel
n	active nucleation site density		
P	pressure (kPa)	*Greek letters*	
P_c	critical pressure (kPa)	ρ	density (kg/m^3)
P_r	reduced pressure (kPa)	σ	surface tension (N/m)
Pr	Prandtl number		
q	heat flux (W/m^2)	*Subscripts*	
R_a	average surface roughness (μm)	c	copper rod
T	temperature (K)	l	liquid phase
T_w	average boiling surface temperature (K)	v	vapor phase
ΔT_s	superheat (K)	sat	saturation
u	uncertainty		

References

[1] Ciloglu, D. and Bolukbasi, A. *A comprehensive review on pool boiling of nanofluids.* Applied Thermal Engineering, 2015. 84: p. 45-63.

[2] Vafaei, S. and T. Borca-Tasciuc, *Role of nanoparticles on nanofluid boiling phenomenon: Nanoparticle deposition.* Chemical Engineering Research and Design, 2014. 92(5): p. 842-856.

[3] Liter S G. and Kaviany M. *Pool-boiling CHF enhancement by modulated porous-layer coating: theory and experiment*. International Journal of Heat & Mass Transfer, 2001, 44(22):4287–4311.

[4] Taylor, R.A. and P.E. Phelan, *Pool boiling of nanofluids: Comprehensive review of existing data and limited new data.* International Journal of Heat and Mass Transfer, 2009. 52(23-24): p. 5339-5347.

[5] Barber, J., D. Brutin, and L. Tadrist, *A review on boiling heat transfer enhancement with nanofluids.* Nanoscale Res Lett, 2011. 6(1): p. 280.

[6] Kshirsagar, J.M. and R. Shrivastava, *Review of the influence of nanoparticles on thermal conductivity, nucleate pool boiling and critical heat flux.* Heat and Mass Transfer, 2014. 51(3): p. 381-398.

[7] Neto A R, Oliveira J L G, and Passos J C. *Heat transfer coefficient and critical heat flux during nucleate pool boiling of water in the presence of nanoparticles of alumina, maghemite and CNTs*. Applied Thermal Engineering, 2017, 111:1493-1506.

[8] Leong K C, Ho J Y and Wong K K. *A critical review of pool and flow boiling heat transfer of dielectric fluids on enhanced surfaces*. Applied Thermal Engineering, 2017, 112:999-1019.

[9] Park, K.-J. and D. Jung, *Enhancement of nucleate boiling heat transfer using carbon nanotubes.* International Journal of Heat and Mass Transfer, 2007. 50(21–22): p. 4499-4502.

[10] Trisaksri, V. and S. Wongwises, *Nucleate pool boiling heat transfer of TiO2–R141b nanofluids.* International Journal of Heat and Mass Transfer, 2009. 52(5–6): p. 1582-1588.

[11] Gerardi, C., et al., *Infrared thermometry study of nanofluid pool boiling phenomena.* Nanoscale Research Letters, 2011. 6(1): p. 1-17.

[12] Vafaei, S., *Nanofluid pool boiling heat transfer phenomenon.* Powder Technology, 2015. 277(0): p. 181-192.

[13] Launay, S., et al., *Hybrid micro-nano structured thermal interfaces for pool boiling heat transfer enhancement.* Microelectronics Journal, 2006. 37(11): p. 1158-1164.

[14] Ujereh, S., T. Fisher, and I. Mudawar, *Effects of carbon nanotube arrays on nucleate pool boiling.* International Journal of Heat and Mass Transfer, 2007. 50(19–20): p. 4023-4038.

[15] White, S.B., A.J. Shih, and K.P. Pipe, *Boiling surface enhancement by electrophoretic deposition of particles from a nanofluid.* International Journal of Heat and Mass Transfer, 2011. 54(19–20): p. 4370-4375.

[16] McHale, J.P., et al., *Pool Boiling Performance Comparison of Smooth and Sintered Copper Surfaces with and Without Carbon Nanotubes.* Nanoscale and Microscale Thermophysical Engineering, 2011. 15(3): p. 133-150.

[17] Tang, Y., et al., *Pool-boiling enhancement by novel metallic nanoporous surface.* Experimental Thermal and Fluid Science, 2013. 44(0): p. 194-198.

[18] Jun, S., S. Sinha-Ray, and A.L. Yarin, *Pool boiling on nano-textured surfaces.* International Journal of Heat and Mass Transfer, 2013. 62(0): p. 99-111.

[19] Lee, C.Y., B.J. Zhang, and K.J. Kim, *Influence of heated surfaces and fluids on pool boiling heat transfer.* Experimental Thermal and Fluid Science, 2014. 59(0): p. 15-23.

[20] Dong, L., X. Quan, and P. Cheng, *An experimental investigation of enhanced pool boiling heat transfer from surfaces with micro/nano-structures.* International Journal of Heat and Mass Transfer, 2014. 71(0): p. 189-196.

[21] Li, Y.-Y., Z.-H. Liu, and B.-C. Zheng, *Experimental study on the saturated pool boiling heat transfer on nano-scale modification surface.* International Journal of Heat and Mass Transfer, 2015. 84: p. 550-561.

[22] Besra, L. and M. Liu, *A review on fundamentals and applications of electrophoretic deposition (EPD).* Progress in Materials Science, 2007. 52(1): p. 1-61.

[23] Deen, I. and I. Zhitomirsky, *Electrophoretic deposition of composite halloysite nanotube–hydroxyapatite–hyaluronic acid films.* Journal of Alloys & Compounds, 2014. 586(4): p. S531-S534.

[24] *http://www.solvay.com/en/markets-and-products/featured-products/SOLKATHERM-SES36.html.*

[25] Fröba, A.P., et al., *Thermophysical Properties of a Refrigerant Mixture of R365mfc (1,1,1,3,3-Pentafluorobutane) and Galden® HT 55 (Perfluoropolyether).* International Journal of Thermophysics, 2007. 28(2): p. 449-480.

[26] Song, G., et al., *Uniform design for the optimization of Al 2 O 3 nanofilms produced by electrophoretic deposition.* Surface & Coatings Technology, 2015. 286: p. 268-278.

[27] Moffat, R.J., *Describing the uncertainties in experimental results.* Experimental Thermal & Fluid

Science, 1988. 1(1): p. 3-17.

[28] Cooper, M.G., *SATURATION NUCLEATE POOL BOILING - A SIMPLE CORRELATION A2 - Simpson, H C*, in *First U.K. National Conference on Heat Transfer*, G.F. Hewitt, et al., Editors. 1984, Pergamon. p. 785-793.

[29] Jones, B.J., J.P. Mchale, and S.V. Garimella, *The Influence of Surface Roughness on Nucleate Pool Boiling Heat Transfer.* Journal of Heat Transfer, 2009. 131(12): p. 315-320.

[30] Mikic, B.B. and W.M. Rohsenow, *A New Correlation of Pool Boiling Data Including the Effect of Heating Surface Characteristics.* Journal of Heat Transfer, 1969. 91(2): p. 245-250.

[31] Wen D S, Wang B X, Effects of surface wettability on nucleate pool boiling heat transfer for surfactant solutions[J]. International Journal of Heat and Mass Transfer, 2002, 45(8):1739-1747.

[32] Klein, S.A., *Engineering Equation Solver.* F-Chart Software, 2010.

Highlights of the Paper

- Nucleate pool boiling of SES36 on nanoporous surfaces obtained by EPD is evaluated
- Three kinds of experiment are performed to compare smooth and nanoporous surfaces
- The HTC increases by 76.9% for a nanoporous surface at heat flux of 90 kW/m^2
- The increased nucleation site density of the nanoporous surface enhances the HTC